Journal Title
XX(X):2–23

DOI: 10.1177/ToBeAssigned
www.sagepub.com/
SAGE

A comparative study into the effects of pre and post catalyst exhaust gas recirculation on the onset of knock

Dominic Parsons[1], Simon Orchard[1], Nick Evans[1], Umud Ozturk[1], Richard Burke[1], Chris Brace[1]

Abstract

Exhaust gas recirculation (EGR) is proven as a valuable technology for controlling knock whilst maintaining lambda one operation, and is also capable of providing efficiency gains at low load. Whilst the evidence supporting the benefits of EGR is unanimous, there is no consensus on optimum EGR strategies amongst the wealth of various possible architectures.

Few studies in the literature address the question of EGR composition effects, namely whether the EGR gas is sourced from before or after the catalyst, and this remains an area which is often overlooked whilst investigating EGR performance.

This paper demonstrates a novel method combining experiment air-path emulation and in-depth data processes to compare the effect of EGR catalysis on the angle of knock onset in a 1L GDI engine. Since initial temperature and pressure have a significant impact on knocking behaviour, an artificial boosting rig replaced the turbomachinery. This enabled fine control over the engine boundary conditions to ensure parity between the catalysed and un-catalysed cases.

To overcome the difficulty of comparing stochastic phenomena in an inherently variable dataset, a pairing method was combined with Shahlari and Ghandhi's angle of knock onset determination method to assess the effects of EGR composition on knock onset for EGR rates ranging from 9% to 18%.

The air path emulation system stabilised the engine combustion to provide a suitably rich dataset for analysing knock using the pairing method. Catalysed EGR improved the mean knock onset angle by 0.55 CAD, but due to the inherent variability in cylinder pressure data this only equated to a 58.3% chance of a later knock onset angle for catalysed EGR in any given pair of comparative cycles.

Prepared using sagej.cls

Keywords
EGR, exhaust gas recirculation, catalysed, knock, combustion, gasoline, GDI

Introduction

More stringent government legislation is a constant driver towards reduced vehicle emissions, and despite the growth of electrification in passenger vehicles, further development of the internal combustion engine is still crucial to achieving these targets.

The potential of the IC engine to realise more efficient operation and reduced emissions lies in the development of several advanced technologies. Modern gasoline engines commonly use direct injection, and have seen a vast trend in downsizing and downspeeding to reduce the friction and pumping losses associated with higher displacement engines.

In order to achieve the power outputs of their larger counterparts downsized engines often use turbocharging to recover waste energy from the exhaust gases and increase their output. This increases the level of component protection that must be employed in certain regions of their operating strategies – both to control knock and to reduce exhaust temperatures to protect the turbomachinery. A common solution for this is to retard the ignition to avoid knocking conditions, and inject excess fuel to cool the exhaust gases. Needless to say, this is harmful to the engine emissions and fuel economy.

There are a number of alternative strategies for controlling knock without the need for overfuelling and EGR is particularly prominent in this area [1, 2]. The dilution effect of EGR can mitigate the risk of knocking combustion at high loads [3] whilst also providing fuel economy benefits at low load by reducing throttling losses [4].

Anticipated CO restrictions in the Euro 7 emissions regulations, alongside the real driving emissions (RDE) test protocols, have added to the pressure on OEMs to realise lambda one operation across the entire operating range of their engines. Whilst EGR is a promising technology in the field, it sits amongst a number of other promising technologies such as variable compression ratios (VCRs), water injection [5], and hybridisation.

[1]University of Bath

Corresponding author:
Dr Dominic Parsons
University of Bath
BA2 7AY
Email: dp255@bath.ac.uk

Prepared using sagej.cls *[Version: 2017/01/17 v1.20]*

Understanding of the effects the EGR has on combustion is essential for accurate modelling studies, and the chemical effect of EGR composition is a rarely considered factor in this.

Until now only a few studies have investigated the impact of the catalyst in EGR operation, and these results are heavily impacted by the turbocharger performance and its sensitivity to changes in pressure differentials.

The aim of this paper is to demonstrate the effect of EGR composition, whether sourced from before or after the catalyst, on the angle of knock onset. In order to fully assess the compositional effects of EGR this experiment has been devised to negate the interactions between the combustion chamber and the turbomachinery. Furthermore a novel method of cycle paring is employed to analyse the effect on more detail whilst taking account for the stochastic nature of knock.

Background

EGR can benefit both high and low load operation in SI engines. At low load the EGR gases displace a proportion of the inlet charge, thereby de-throttling the engine without the associated losses of mechanical throttling.

At high load EGR can advance knock limits, thereby allowing stoichiometric combustion closer to maximum brake torque (MBT) spark timing. This can offer both improved efficiency and also reduced NO_X emissions due to lower combustion temperatures.

EGR architectures

EGR systems can take a number of different forms of varying complexity. The location of its source and delivery points in relation to the turbocharger define the architecture of an EGR system, the two most common architectures being low pressure (LP – shown in Figure 1a) and high pressure (HP – shown in Figure 1b). The former sources the EGR gases from after the turbine, and delivers them pre-compressor. The latter sources them from before the turbine and delivers them post-compressor. Mixed pressure architectures are also possible but are less common. The one overruling requirement is a positive pressure differential between the source and delivery locations of the EGR system, and this can be a limiting factor at some operating conditions.

A large number of studies have assessed the potential of EGR in each of these architectures [6–19], with some researchers advocating the combination of both high pressure and low pressure EGR architectures to allow full map operation of the EGR system without the obstacles associated with each individual architecture [4].

Additional factors in the design of EGR systems include the potential for condensate to damage the compressor in LP architectures, and additional demands that cooled EGR can place on vehicle cooling systems.

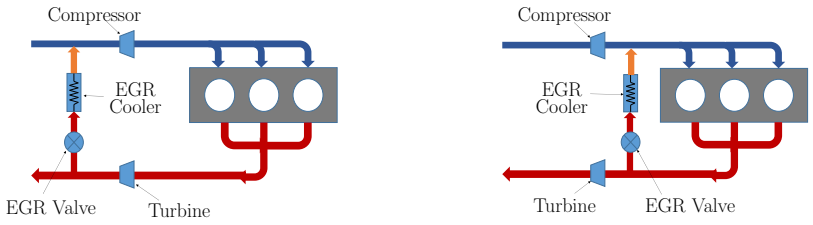

(a) **(b)**

Figure 1. Schematic of low pressure (a) and high pressure (b) EGR architectures

Catalysed EGR

The conversion of NO_X, CO and HCs into N_2, CO_2 and H_2O in a catalyst reduces the number of chemically active ingredients in EGR, thereby altering the availability of radicals in the end gas during combustion relative to pre-catalyst EGR.

Several studies investigate the use of a catalysed EGR system in an LP architecture without any mention of the chemical significance of this and without any comparison of performance between the catalysed loops and equivalent uncatalysed loops [4, 7, 16]. Only a few examples can be found in the literature where this kind of comparison has been made.

Roth et al [20] considered the advantages of operating an SI engine with BMEP values reaching 17 bar with both LP and HP EGR configurations available to cover the full operating range. Within this study the authors experimentally compared the effect of post catalyst versus pre catalyst EGR for the LP loop. They concluded that pre-catalyst EGR was preferable to catalysed EGR because:

- The average BSFC was improved by 1.5-3.5%, with a higher power production observed for all points despite having up to 5°CA less favourable combustion phasing due to knock.
- The combustion rate was faster.
- HC emissions were lower by 30-40%.
- PMEP was reduced by 5-15% at higher speeds and loads.
- The pressure differential available to drive the EGR was larger due to the pressure loss over the catalyst, allowing a reduced EGR valve size and larger delivery range.

Roth et al [20] do mention that a significant amount of internal EGR, which is of course uncatalysed, was present at some of their test points and therefore could have affected the data produced. At a reference 10% external EGR rate they record an internal EGR fraction from 8% up to 48%, dependent on speed,

load, and valve timing. This could lead to a potentially significant quantity of NO content in the cylinder, which could impact the comparison between the EGR compositions.

In contrast to Roth et al's study [20], Hoffmeyer et al [21] found an improvement in fuel consumption of up to 2% with the catalysed EGR compared to that of the non-catalysed loop, which they attribute to earlier combustion phasing (1.5 - 3°CA) as a result of the increased knock tolerance of the engine. They cite the increased heat capacity of the inlet charge due to the increased CO_2, and the reduction of NO and HCs after catalysis as the primary reasons for the increased knock limit. The disparity between the findings of these two studies highlights the difficulty in achieving a fair comparison between the two EGR compositions. Inlet temperature and pressure cannot be controlled accurately whilst using a turbocharger and can have a significant impact on knocking behaviour. Additionally, engine operating conditions can impact the minor species concentrations in the exhaust, which in turn affects the impact of catalysis.

In addition to their experimental work Hoffmeyer et al analysed the chemical interactions using a reduced PRF mechanism (from [22] – 233 species, 2019 reactions) blended with an early version of the GRI-Mech NO sub-model [23] in a homogeneous reactor model. A sensitivity study based on this model highlighted NO and C_2H_2 as the main protagonists in shortening ignition delay time for uncatalysed EGR.

More recently, research has been conducted at the University of Bath by Lewis et al [24] on an SI engine with BMEP levels reaching 26.5 bar and a catalyst installed in the EGR loop. Concerns over errors introduced by measuring the EGR rate via the CO_2 ratio between the inlet and exhaust manifolds prompted them to use the mass air flow into the engine as a measure instead. This means that their investigation is carried out with a constant total air flow into the engine (air + EGR) rather than a constant load on the engine and, as such, the load and fuelling decreases with higher EGR rates due to the reduction in oxygen in the charge and the ECU being set to maintain stoichiometry.

Lewis et al [24] found an increase in the knock limit of up to 6°CA with catalysed EGR for equivalent EGR mass flows, but at equivalent BMEP values the BSFC was found to increase by up to 10%. This is attributed to the lower calorific value of the charge for catalysed EGR due mainly to the oxidation of HCs and CO in the catalyst. One significant point from their study is that the engine-out CO and HC emissions were considerably higher than would be expected for stoichiometric in-cylinder operation. They concluded that this was due to the blow-through of fresh air due to valve timing overlaps, causing the engine to be running rich in-cylinder despite the exhaust lambda sensors showing it to be running at stoichiometry. Another effect of rich in-cylinder conditions is that NO_X emissions are relatively low, so the catalysis of the exhaust gases in this study would have offered little benefit from the reduction in EGR NO_X content.

The consensus in the literature supports the removal of NO as the primary influencer in potentially improving knock limits with catalysed EGR. NO is a highly reactive substance and as such can have a significant impact on the combustion process. A large number of investigations have been performed to assess the volatility of NO addition to C_1-C_2 hydrocarbons [25–29], and to C_3-C_5 hydrocarbons [25, 30–32]. Further studies into the NO sensitisation effect on the larger hydrocarbon compounds that are used to make up gasoline surrogates have revealed a high sensitivity to initial temperature, fuel composition and NO concentration [33–39], often attributed to octane ratings and NTC behaviour.

NO mechanisms

NO is known to promote a more rapid build-up of the radical pool [40], most notably with the production of reactive OH radicals. An abundance of these radicals can increase the reactivity of the end gas and therefore the propensity for autoignition to occur.

The mechanism by with NO promotes the production of OH radicals are shown in reaction 1:

$$NO + HO_2 \rightarrow NO_2 + OH \tag{1}$$

NO is also formed from NO_2 by:

$$NO_2 + H \rightarrow NO + OH \tag{2}$$

The net effect of reactions 1 and 2 is:

$$HO_2 + H \rightarrow 2OH \tag{3}$$

which is more active than the recombination reaction:

$$HO_2 + H \rightarrow H_2O_2 \tag{4}$$

An inhibitory effect of NO at high concentrations has also been observed [40], which indicates the presence of competing reaction paths that consume radicals during combustion. The following mechanisms, published by a number of researchers [34, 35, 38, 40, 41], describe this process:

The scavenging of OH radicals can occur by:

$$NO + OH + [M] \rightarrow HONO + [M] \tag{5}$$

$$HONO + OH \rightarrow NO_2 + H_2O \tag{6}$$

These two equations effectively equate to:

$$NO + 2OH \rightarrow NO_2 + H_2O \tag{7}$$

In addition, NO_2 can scavenge peroxy radicals (HO_2) to form HONO, which then consumes more OH radicals:

$$NO_2 + HO_2 \rightarrow HONO + O_2 \tag{8}$$

The inhibiting effect is the result of both the competition between reactions 8 and 1 and the chain termination effect of reaction 6.

Combustion pathways in the high temperature regime (>1000K) seem less affected by NO [40] as alternative production paths for OH radicals become more active. This limits the impact of NO to the earlier stages of combustion where autoignition is more prevalent, whilst not having a significant effect on combustion duration or exhaust temperature [38].

Cyclic variability considerations

Cyclic variability is inherent to engine combustion and is a topic that has previously received attention due its impact on engine driveability and efficiency [42, 43]. The most common measure of cyclic variability is the coefficient of variance (CoV) of the IMEP, defined as:

$$\mathrm{CoV}_{\mathrm{IMEP}} = \frac{\sigma_{\mathrm{IMEP}}}{\mu_{\mathrm{IMEP}}} \tag{9}$$

Target values for CoV vary in the range of 2-10%, depending on the application, but modern engines typically sit towards the lower end of this range [44].

EGR is known to increase the cyclic variability of gasoline engines, in most part due to the decreased burn rates that are associated with EGR [45].

Since knocking combustion is heavily impacted by end gas conditions, cyclic variability is an important factor to consider whilst making comparisons between different conditions. The cycle pairing method demonstrated in this study was designed to overcome the challenges of comparing inherently variable data.

Summary

The current literature provides evidence that catalysed EGR may offer increased knock inhibition over uncatalysed EGR due to the reduction in NO content, but there is no conclusive evidence of the fuel consumption benefits due to the overarching effects of varying architectures and turbocharger performance. Lewis et al [24] circumvent these issues by using an artificial boosting system, but by their own admission the results are skewed by inconsistent catalyst light-off and excessive blow-through allowing the uncatalysed EGR to contain a significant quantity of oxygen.

The experimental process for this study aims to achieve consistent and stable engine boundary conditions to allow a more accurate comparison between the two EGR compositions. These consistent conditions will enable the use of a cycle pairing method to negate the effects of cyclic variation and give a true representation of the knock onset effects.

Table 1. Table of engine details

Engine Type	In-line 3 cylinder, 4 valves per cylinder
Engine displacement (cm^3)	999
Bore/Stroke (mm)	71.9/82
Compression ratio	10.5:1
Firing Order	1-2-3
Valve train	Dual continuously variable camshaft phasers
Rated power(kW/l)	92 @ 6000 rpm
Rated torque(Nm/l)	170 @ 1400-4500 rpm
Other	External cooled EGR Water cooled exhaust manifold

Methodology

Inlet pressure and temperature can have a significant impact on knocking behaviour and cannot be controlled accurately in a typical engine with a turbocharger, which can be affected by even small changes to ignition timing or EGR rate. For this experiment the engine turbocharger is removed and combustion air and engine back pressure are provided by an artificial boosting rig.

Since the boost rig removed any potential low pressure delivery point for the EGR gases, an additional rig was required to deliver the EGR gases to the inlet side, as illustrated in Figure 2. Further details of the hardware are provided in [46].

The engine

The investigations in this chapter were performed on a production 1 litre GDI engine. For this testing the inlet and exhaust valve phasing was kept constant to maximise the consistency of combustion conditions for each test point. The valve phasing was decided by an initial sweep to find the maximum possible overlap before the exhaust oxygen content began to rise. 1D simulations performed on a full engine model in GT Power predicted a residual content of 2.9% for these conditions. Further details of the engine are given in Table 1.

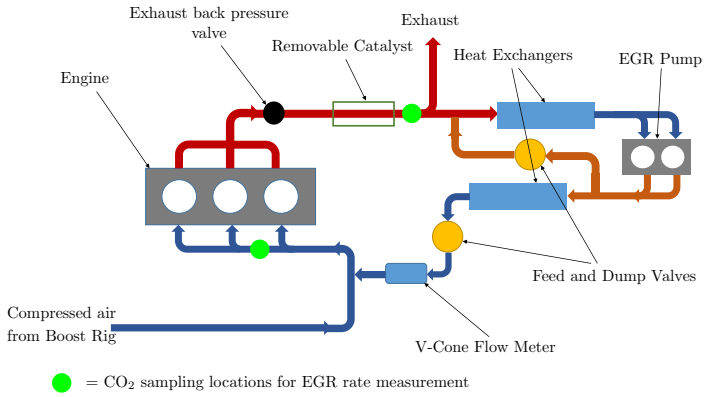

Figure 2. Schematic of the engine and EGR rig setup

Test cell facilities

The test cell was equipped with an artificial boost rig which provided compressed dry air to the inlet manifold of the engine. The main operating parts of the boost rig are illustrated in Figure 3.

A 7 bar supply of dry compressed air was filtered and regulated down to 3.5 bar. A heater on closed loop control regulated the temperature of the air, with the feedback coming from a thermocouple installed in the engine manifold. The air supply to the engine was throttled to maintain the required manifold pressure and excess air was released through a dump valve.

The back pressure that would be present with turbomachinery installed was emulated by an exhaust back pressure valve, which could maintain a target back pressure for steady state running.

The mass airflow was measured by two Sierra 'FastFlo' thermal gas flow meters, one measuring total flow into the rig and the other measuring the flow to the engine. The dump flow was calculated by the difference of these two values. During the test programme it was observed that the engine airflow values were not consistent across equivalent operating points. The culprit for this was identified as the accuracy of the flow meters measuring the mass of air expelled from the rig. Since the available time and funding for this project did not allow for replacement of these flow meters, the engine airflow was instead calculated by the fuel flow and combustion stoichiometry during post-processing. Details of the measurement systems in the test cell are included in Table 2.

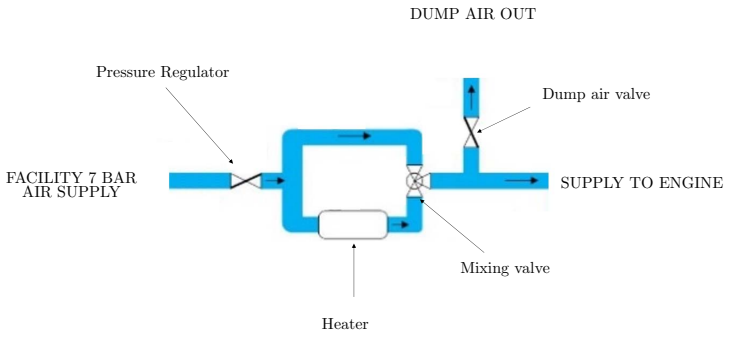

Figure 3. Schematic of the boost rig. The air temperature is regulated by the heater power and bypass airflow.

Table 2. Table of test cell facilities

Dynamometer	300 kW AC dynamometer
Speed measurement	1024 pulse/rev encoder
Torque measurement	1 kNm torque measurement flange
Combustion analysis	AVL X-ion 6 channel system Kistler 3600 pulse/rev optical encoder Kistler 6054A in-cylinder transducers sampling every 0.1 CAD Kistler 4049A water-cooled exhaust pressure transducer Kistler transducer cooling module and amplifiers
Fuel flow measurement	CP Engineering FMS-1000 1 litre gravimetric fuel meter
Emissions	2 off MEXA 7100 DEGR exhaust gas analysers for simultaneous pre and post-catalyst sampling of CO_2, CO, HC, O_2, NO_X
AFR	UEGO lambda sensor
Other measurements	Up to 32 K-type thermocouples, 16 PRTs and 16 pressure channels, coolant flow rate (Krone magnetic flow meter)

The EGR rig

The EGR rig comprises of a 600 cm^3 engine which was used as a positive displacement compressor to drive the EGR flow, motored by an 11kW three

phase induction motor. Two ball valves controlled a recirculation loop in the rig, allowing more precise control of the compressor outlet pressure and delivery rate of EGR gases to the inlet. The layout of the rig is included in Figure 2.

A heat exchanger was positioned before the EGR compressor to cool the incoming exhaust gases, with a secondary heat exchanger positioned in the feed line from the EGR compressor. The compressor and the secondary heat exchanger were connected to the coolant supply of the test engine in an attempt to regulate both the compressor oil temperature and the feed EGR gas temperature.

To avoid issues with catalyst light-off, the catalyst was positioned closer to the engine and before the sampling point for the EGR rig. A blank pipe section replaced the catalyst for the pre-catalyst EGR test points.

The ratio of the CO_2 concentrations between the feed gas and the inlet manifold (measurement locations detailed in Figure 2) were used to calculate the EGR rate.

The experimental setup is described in more detail in [46].

Testing Procedure

A warm-up procedure was followed for both the engine and the EGR compressor to allow the oil and coolant to warm up to their target values, which were maintained via PID controlled heat exchangers once they had been reached. Repeatability points were taken at the start and end of each test session to confirm the consistency of the test data.

The manifold pressure was fixed at 1.7 bar(abs) for this experiment, and spark sweeps were performed at EGR rates from 9% to 18% at an engine speed of 2200 rpm, as detailed in Table 3. A knock histogram in AVL Indicom defined the knock threshold for advancing the spark angle.

The cam phasing was adjusted to provide the maximum allowable overlap without the oxygen content exceeding that measured for no overlap, in an effort to maximise scavenging without excessive blow-through. The cams were then fixed at these positions for the duration of the experiment. Fuel pressure was fixed at 172 bar, injection timing was fixed at 300°CA, lambda 1 operation was maintained for the experiment and the intake temperature was fixed at 30°C via a PID control on a heater and bypass in the boost rig. The exhaust pressure was fixed at 1.5 bar by way of a cable controlled back pressure valve.

Method of comparison of knock onset angles

Table 3. Table of experimental conditions

EGR composition	Pre/post catalyst
External EGR rate (%)	9-18
Speed (rpm)	2200
Fuel RON	95
Fuel Pressure (bar)	172
Injection timing (°CA)	300
Inlet manifold pressure (bar (abs))	1.7
Exhaust manifold pressure (bar (abs))	1.5
Intake temperature (°C)	30

Comparing like-for-like cylinder pressure traces can be difficult with multi-cylinder engines, due to the variation between cylinders causing some uncertainty on the exact charge composition distribution. For this reason a method was devised to directly compare cycles with the same initial conditions, as identified by the cylinder pressure data. By this method the effect of cycle-to-cycle variations was minimised in an attempt to isolate the charge composition effects on knock. All of the knock onset data for this analysis was taken from cylinder 2, as it was the most prone to knock so gave the highest number of knocking cycles for comparison.

- to minimise error, comparative data points were chosen from the data where the inlet port temperature difference did not exceed 1°C (six conditions were found to be within this range whilst also providing at least 15 knocking cycles – these six conditions are detailed in Table 4).
- only cycles with a knock index (for this the maximum amplitude of pressure oscillations was used (MAPO)) exceeding 0.5 bar were selected, so that comparisons were being made between cycles that were actually knocking
- since the post catalyst conditions always showed fewer knocking cycles than their equivalent pre catalyst EGR condition, for each of the knocking post-cat EGR cycles a least square difference was performed between that cycle and all of the knocking pre-cat EGR cycles in the "curve matching region" (from IVC until 10°CA ATDC – shown by the shaded area in Figure 4) to capture the deviation during the compression stroke and initial flame kernel growth. The pre-cat cycle that was the closest match was then paired up with that post-cat cycle, any paired cycles with a root mean squared error (RMSE) over the threshold of 0.1 bar were discarded. This way it was hoped that the comparison would be made for cycles with sufficiently equivalent initial conditions.
- knock onset was calculated for each of the cycles by the signal energy ratio (SER) method of Shahlari and Ghandhi [47] – this method calculates

the signal energy of the pressure oscillations (SEPO) at each crank angle step by integration of the filtered pressure oscillations. The SER is then calculated by the square of the "forward" integral of the pressure oscillations over the following 5 crank angle degrees (SEPO_{fwd}), divided by the square root of the "backward" integral of the pressure oscillations over the previous 5 crank angle degrees (SEPO_{bwd}). This is more clearly described by Equation 10:

$$\mathrm{SER} \equiv \frac{\mathrm{SEPO}_{fwd}^2}{\mathrm{SEPO}_{bwd}^{1/2}} = \frac{\left(\int_{\theta_0}^{\theta_0+\Delta\theta} P_{filt}^2 d\theta\right)^2}{\left(\int_{\theta_0-\Delta\theta}^{\theta_0} P_{filt}^2 d\theta\right)^{1/2}} \tag{10}$$

P_{filt} in this case is the band filtered pressure trace isolating the strongest harmonic oscillation ($f_{most-energy} \pm 1.5$kHz) – identified by examination of the power spectral density (PSD) for that cycle. This band has been highlighted in the bottom two plots of Figure 4. Whilst most commonly seen at the first harmonic mode, as is the case for the two illustrative cycles, this is not always the case.

- the knock onset timing for each of the pairs was compared, and the difference between the two knock set angles in each pair makes up the data for Figure 5.

Table 4. Table of conditions analysed for knock onset comparison. These test points passed the criteria for inlet temperature and sufficient number of knocking cycles for both the pre and post catalyst tests.

EGR rate (%)	Spark angle (CAD BTDC)	IMEP (bar)
9	4.0	19.5
12	6.0	19.2
15	6.5	18.8
15	7.0	18.9
18	8.5	18.6
18	9.0	18.6

Figure 4 illustrates this method by displaying a comparison of one of the pairs of cycles – the post-catalyst cycle on the left and the pre-catalyst cycle on the right. The shaded region in the top two plots denotes the part of the cycle which was considered in matching corresponding cycles for comparison.

The knock onset angle, denoted by the dashed black line in all plots, is demonstrated to be fairly accurate when compared to the band pass filtered traces (middle row). The SER is included in this plot to reveal how the SER value evolves with increasing crank angle. The method of calculating the SER uses only the most powerful harmonic frequency – with Shahlari and Ghandi

reporting that this reduces erroneous results due to the less well defined peak in the SER function that occurs when all frequencies are included in the signal to be analysed.

The pre-cat EGR cycle shows some well defined oscillations at the first resonant mode very early in the cycle, which are not powerful enough to qualify as knock. For this cycle the knocking pressure oscillations occur much later in the cycle at a higher resonance mode, which indicates the presence of sub-knocking autoignition preceding the initiation of knocking combustion for this cycle.

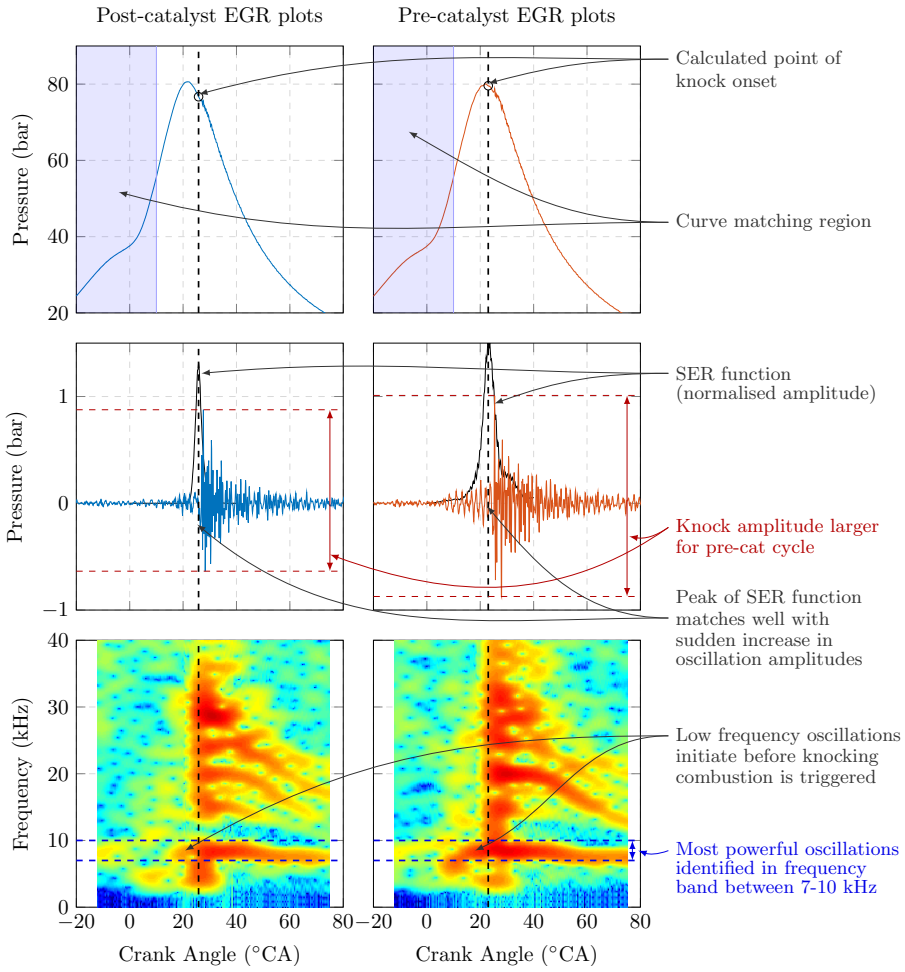

Figure 4. An illustration of the analysis method for comparing the angle of knock onset. From top to bottom these plots illustrate: cylinder pressure traces, filtered pressure trace (4 - 35 kHz band pass filter), power spectral density heat map showing oscillation power as a function of crank angle and frequency. These plots were taken from a pair of cycles at 15% EGR with a spark angle of 7 degrees BTDC.

Results and discussion

The comparison method produced 229 pairs of cycles across the six different conditions. Figure 5 illustrates the distribution of knock onset deltas for the paired cycles. Box plots have been selected to display this data to give a representation of the distribution of the data at each condition. The boxes illustrate the median and upper and lower quartiles for the data, and the whiskers extend to the furthest data points within 1.5 times the inter-quartile range above and below the upper and lower quartiles respectively. Outliers are

represented by the circles beyond this range. Whilst the results do tend to show slightly later knock onset for post-cat EGR, the difference is not statistically significant at a 95% confidence level.

The mean improvements at each equivalent condition range from an improvement of 1.9 °CA down to an improvement of just 0.25 °CA, but with standard deviations in the region of 2 to 3 degrees.

The data from Figure 5 suggests that at a given condition the probability of autoignition being delayed with post-cat EGR relative to pre-cat EGR is slightly higher – the mean improvement is 0.55°CA. The relatively high standard deviation of the differences means that, if assuming a normal distribution, for a given pair of cycles only 58.3% would be expected to show a later angle of knock onset for catalysed EGR. The significance of the onset angle is relevant to the modelling realm, where onset angles are often predicted by knock models. Experimental evaluation is therefore most applicable to model validation.

Comparing the data displayed in Figure 5 for the two ignition angles at 15% EGR and likewise at 18% EGR shows a noticeable reduction in change of knock onset angle when the spark is advanced a further 0.5°CA. A reduction in the knock onset delay enabled by EGR catalysis for more advanced spark angles may indicate that at conditions further beyond the knock limit there is an abundance of reactive radicals in the end gas regardless of the presence of NO, therefore reducing the impact that NO has. The data, however, does not provide statistically significant evidence for this phenomenon whilst there are only two points for comparison.

A later onset of knock would usually be expected to result in lower knock intensities due to the reduction in cylinder pressure and unburned mass. Despite this dataset not showing a statistically significant change in onset angle for the change in EGR composition, the knock amplitudes are higher for the pre-cat EGR condition. This is illustrated in Figure 4 for the pair of cycles selected, but also becomes quite apparent when comparing the knock intensity values for the pairs as shown in Figure 6.

These results suggest that the effect of removing the minor species from EGR can reduce the intensity of autoignition events whilst having minimal impact on delaying their onset angle. The mechanisms for this increase in intensity are likely related to the reaction paths involved with NO sensitisation of hydrocarbon oxidation, which may increase the abundance of reactive radicals in the end gas.

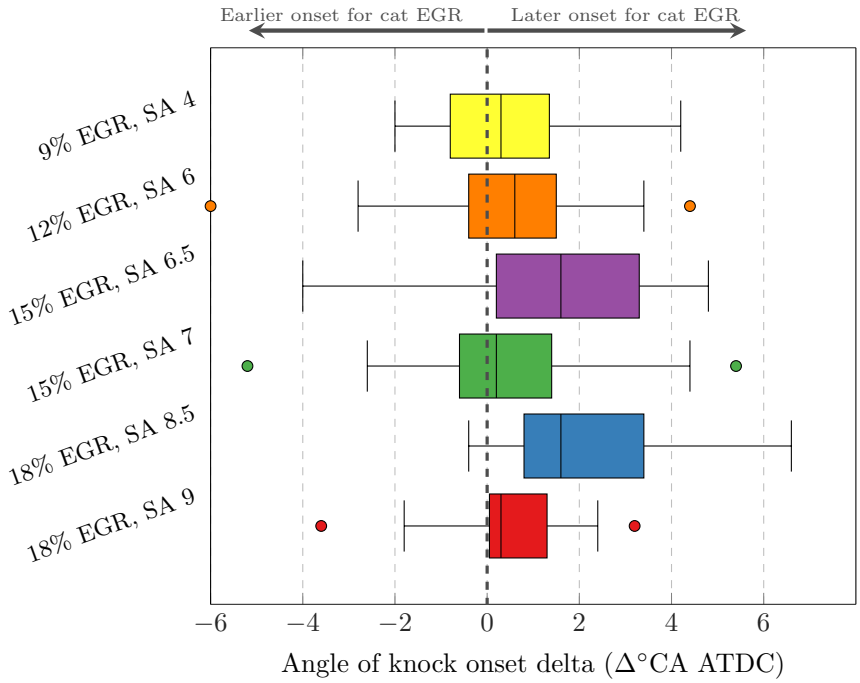

Figure 5. Box plot showing the distribution of the knock onset angle difference between equivalent pre and post-catalyst EGR pairs. Although the angle of knock onset seems to generally be more retarded for catalysed EGR conditions – particularly at higher EGR rates – there is a large spread in the data, with a large overlap between pre and post-catalyst values. Spark angles are given in degrees BTDC.

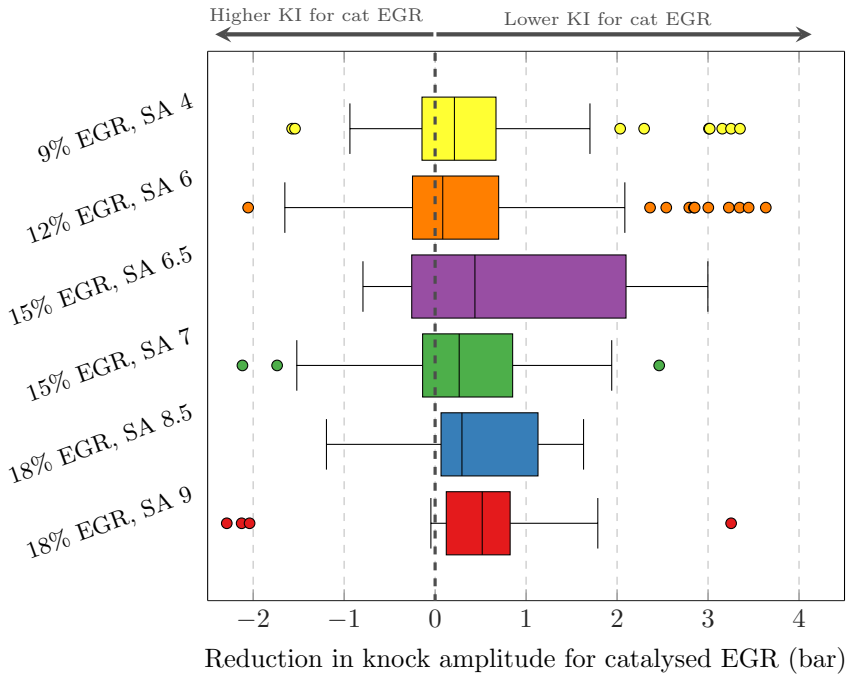

Figure 6. A comparison of the knock intensity between equivalent pre and post-catalyst EGR pairs. The data shows an average reduction in knock intensity of 0.4 bar for equivalent cycles. Spark angles are given in degrees BTDC.

Conclusions

This study has demonstrated an experimental setup to enable a direct comparison between the effects pre and post catalyst EGR on the angle of knock onset in a GDI engine. The inherent variability in SI combustion presents obstacles to the direct comparison of different conditions, so a pairing method has been devised to overcome this. In combination with the method devised by Shahlari and Ghandhi for assessing the knock onset angle from a pressure trace this has provided a picture of how the change in EGR composition by catalysis affects the knock onset angle for equivalent conditions. Despite the strictly defined boundary conditions for the cylinder, there is still a significant variance in the knock onset data due to the stochastic nature of knocking combustion, and this is reflected in the standard deviations of the results. The cycle pairing method reveals a probability of 58% that the knock onset angle will be later for catalysed EGR when compared to an equivalent cycle with uncatalysed EGR, the average reduction in knock intensity is 0.4 bar for equivalent cycles.

Combustion modelling methods generally identify knocking cycles by identification of a knock onset angle, the results of this study show a disparity between the onset angles and knock intensity for changing charge composition.

Acknowledgements

This work was conducted under the Advanced Propulsion Centre (UK) project Dynamo, with funding from Innovate UK under grant number 113130.

References

[1] Bozza F, De Bellis V and Teodosio L. Potentials of cooled EGR and water injection for knock resistance and fuel consumption improvements of gasoline engines. Applied Energy 2016; 169: 112–125. DOI:10.1016/j.apenergy.2016.01.129. URL `http://linkinghub.elsevier.com/retrieve/pii/S0306261916301179`.

[2] Keller M, Geiger S, Günther M et al. Model predictive air path control for a two-stage turbocharged spark-ignition engine with low pressure exhaust gas recirculation. International Journal of Engine Research 2020; DOI: 10.1177/1468087420936398.

[3] Franken T, Mauss F, Seidel L et al. Gasoline engine performance simulation of water injection and low-pressure exhaust gas recirculation using tabulated chemistry. International Journal of Engine Research 2020; DOI:10.1177/1468087420933124.

[4] Alger T, Chauvet T and Dimitrova Z. Synergies between High EGR Operation and GDI Systems. SAE International 2008; DOI:2008-01-0134.

[5] Khatri J, Sharma N, Dahlander P et al. Effect of relative humidity on water injection technique in downsized spark ignition engines. International Journal of Engine Research 2020; DOI:10.1177/1468087420940854.

[6] Vitek O, Macek J, Polasek M et al. Comparison of Different EGR Solutions. SAE International 2008; : 776–790DOI:2008-01-0206.

[7] Potteau S, Lutz P, Leroux S et al. Cooled EGR for a Turbo SI Engine to Reduce Knocking and Fuel Consumption. SAE International 2007; DOI: 2007-01-3978.

[8] Turner JWG, Pearson RJ, Curtis R et al. Effects of Cooled EGR Routing on a Second-Generation DISI Turbocharged Engine Employing an Integrated Exhaust Manifold. SAE International 2009; DOI:2009-01-1487.

[9] Galloni E, Fontana G and Palmaccio R. Numerical analyses of EGR techniques in a turbocharged spark-ignition engine. Applied Thermal Engineering 2012; 39: 95–104. DOI:10.1016/j.applthermaleng. 2012.01.040. URL `http://linkinghub.elsevier.com/retrieve/pii/S1359431112000592`.

[10] Hattrell T, Sheppard CGW, Burluka AA et al. Burn Rate Implications of Alternative Knock Reduction Strategies for Turbocharged SI Engines. SAE International 2006; DOI:2006-01-1110.

[11] Fontana G and Galloni E. Experimental analysis of a spark-ignition engine using exhaust gas recycle at WOT operation. Applied Energy 2010; 87(7): 2187–2193. DOI:10.1016/j.apenergy.2009.11.022. URL `http://linkinghub.elsevier.com/retrieve/pii/S0306261909005091`.

[12] Grandin B and Ångström He. Knock Suppression in a Turbocharged SI Engine by Using Cooled EGR. SAE International 1998; DOI:982476.

[13] Grandin B and Ångström He. Replacing Fuel Enrichment in a Turbo Charged SI Engine : Lean Burn or Cooled EGR Reprinted From : Combustion and Emission Formation in SI Engines. SAE International 1999; DOI:1999-01-3505.

[14] Cairns A, Fraser N and Blaxill H. Pre Versus Post Compressor Supply of Cooled EGR for Full Load Fuel Economy in Turbocharged Gasoline Engines. SAE International 2008; DOI:2008-01-0425.

[15] Kaiser M, Krueger U, Harris R et al. Doing More with Less - The Fuel Economy Benefits of Cooled EGR on a Direct Injected Spark Ignited Boosted Engine. SAE International 2010; DOI:2010-01-0589.

[16] Bourhis G, Chauvin J, Gautrot X et al. LP EGR and IGR Compromise on a GDI Engine at Middle Load. SAE International 2013; DOI:2013-01-0256.

[17] Hoepke B, Jannsen S, Kasseris E et al. EGR Effects on Boosted SI Engine Operation and Knock Integral Correlation. SAE International 2012; : 547–559DOI:10.4271/2012-01-0707. URL `http://www.sae.org/technical/papers/2012-01-0707`.

[18] Zhong L, Musial M, Reese R et al. EGR Systems Evaluation in Turbocharged Engines. SAE International 2013; DOI:10.4271/2013-01-0936. URL `http://papers.sae.org/2013-01-0936/`.

[19] Chao Y, Lu H, Hu Z et al. Comparison of Fuel Economy Improvement by High and Low Pressure EGR System on a Downsized Boosted Gasoline Engine. SAE Technical Papers 2017; DOI:10.4271/2017-01-0682.

[20] Roth DB, Keller P and Becker M. Requirements of External EGR Systems for Dual Cam Phaser Turbo GDI Engines. SAE International 2010; DOI:2010-01-0588.

[21] Hoffmeyer H, Montefrancesco E, Beck L et al. CARE – CAtalytic Reformated Exhaust Gases in Turbocharged DISI-Engines. SAE International 2009; : 139–148DOI:2009-01-0503.

[22] Ahmed SS, Moréac G, Zeuch T et al. Reduced Mechanism for the Oxidation of the Mixtures of n-Heptane and iso-Octane. Proceedings of the European Combustion Meeting 2005; .

[23] Smith GP, Golden DM, Frenklach M et al. GRI-Mech 3.0. URL `http://www.me.berkeley.edu/gri{_}mech/`.

[24] Lewis A, Akehurst S, Turner J et al. Observations on the measurement and performance impact of catalyzed vs . non catalyzed EGR on a heavily downsized DISI engine. SAE International 2014; DOI:2014-01-1196.

[25] Frassoldati A, Faravelli T and Ranzi E. Kinetic modeling of the interactions between NO and hydrocarbons at high temperature. Combustion and Flame 2003; 135: 97–112. DOI:10.1016/S0010-2180(03)00152-4.

[26] Glarborg P, Alzueta MU, Dam-Johansen K et al. Kinetic Modeling of Hydrocarbon/Nitric Oxide Interactions in a Flow Reactor. Combustion and Flame 1998; 115(1-2): 1–27.

[27] Dagaut P, Lecomte F, Chevailler S et al. The reduction of NO by ethylene in a jet-stirred reactor at 1 atm: Experimental and kinetic modelling. Combustion and Flame 1999; 119(4): 494–504. DOI:10.1016/S0010-2180(99)00075-9.

[28] Amano T and Dryer FL. Effect of Dimethyl Ether, NOx and Ethane on CH4 Oxidation: High Pressure, Intermediate-Temperature Experiments and Modelling. Twenty-seventh International Symposium on Combustion 1998; : 397–404.

[29] Dagaut P and Nicolle a. Experimental study and detailed kinetic modeling of the effect of exhaust gas on fuel combustion: mutual sensitization of

the oxidation of nitric oxide and methane over extended temperature and pressure ranges. Combustion and Flame 2005; 140(3): 161–171. DOI:10.1016/j.combustflame.2004.11.003. URL http://linkinghub.elsevier.com/retrieve/pii/S0010218004002287.

[30] Glaude PA, Marinov N, Koshiishi Y et al. Kinetic modeling of the mutual oxidation of NO and larger alkanes at low temperature. Energy and Fuels 2005; 19(5): 1839–1849. DOI:10.1021/ef050047b.

[31] Hori M, Matsunaga N, Marinov N et al. An experimental and kinetic calculation of the promotion effect of hydrocarbons on the NO-NO2 conversion in a flow reactor. 27th Symposium on Combustion 1998; : 389–396.

[32] Dagaut P, Luche J and Cathonnet M. Reduction of NO by n -Butane in a JSR: Experiments and Kinetic Modeling. Energy & Fuels 2001; 14(3): 712–719. DOI:10.1021/ef990252p.

[33] Burluka AA, Liu K, Sheppard CGW et al. The Influence of Simulated Residual and NO Concentrations on Knock Onset for PRFs and Gasolines Reprinted From : SI Engine Experiment and Modeling. SAE International 2004; DOI:2004-01-2998.

[34] Prabhu SK, Li H, Miller DL et al. The Effect of Nitric Oxide on Autoignition of a Primary Reference Fuel Blend in a Motored Engine. SAE International 1993; DOI:932757.

[35] Risberg P, Johansson D, Andrae J et al. The Influence of NO on the Combustion Phasing in an HCCI Engine. SAE International 2006; DOI:2006-01-0416.

[36] Naik CV, Puduppakkam K and Meeks E. Modeling the Detailed Chemical Kinetics of NOx Sensitisation for the Oxidation of a Model fuel for Gasoline. SAE International 2010; : 556–566DOI:2010-01-1084.

[37] Roberts PJ and Sheppard CGW. The Influence of Residual Gas NO content on Knock Onset of Iso-octane , PRF , TRF and ULG Mixtures in SI Engines. SAE International 2013; : 1–22DOI:2013-01-9046.

[38] Stenlaas O, Einewall P, Egnell R et al. Measurement of Knock and Ion Current in a Spark Ignition Engine with and without NO Addition to the Intake Air Reprinted From : SI Combustion. SAE International 2003; DOI:2003-01-0639.

[39] Chen Z, Yuan H, Foong TM et al. The impact of nitric oxide on knock in the octane rating engine. Fuel 2019; 235: 495–503. DOI:10.1016/j.fuel.2018.08.039. URL https://doi.org/10.1016/j.fuel.2018.08.039.

[40] Faravelli T, Frassoldati A and Ranzi E. Kinetic modeling of the interactions between NO and hydrocarbons in the oxidation of hydrocarbons at low temperatures. Combustion and Flame 2003; 132: 188–207.

[41] Dubreuil A, Foucher F and Mounaim-Rousselle C. Effect of EGR Chemical Components and Intake Temperature on HCCI Combustion Development. SAE International 2006; : 776–790DOI:2006-32-0044.

[42] Heywood JB. Internal Combustion Engine Fundamentals. McGraw-Hill Inc., 1988.

[43] Stone R. Introduction to Internal Combustion Engines. Third ed. Palgrave Macmillan, 1999.

[44] Matthias N, Wallner T and Scarcelli R. Analysis of Cyclic Variability and the Effect of Dilute Combustion in a Gasoline Direct Injection Engine. SAE International Journal of Engines 2014; 7(2): 633–641. DOI:10.4271/2014-01-1238.

[45] Chappell E, Brace C and Tiley R. Analysis of cyclic variability in gasoline engines. In ASME 2012 Internal Combustion Engine Division Spring Technical Conference. pp. 1–15.

[46] Orchard S, Ozturk U, Evans N et al. A Novel Air and EGR Emulation Facility For The Optimisation Of The Powertrain Architecture. In Proceedings of the ASME.

[47] Shahlari AJ and Ghandhi JB. A Comparison of Engine Knock Metrics. SAE International 2012; DOI:10.4271/2012-32-0007. URL `http://papers.sae.org/2012-32-0007/`.